APPLICATION OF SCATTER CORRECTION TECHNIQUES IN SMALL ANIMAL SPECT IMAGING

E. Karali,* G. Loudos*, N. Sakelios*, K.S. Nikita* and N. Giokaris**
*School of Electrical and Computer Engineering National Technical University of Athens Iroon Politechniou 9, Zografos 15780, HELLAS
**Department of Physics National Kapodistrian University of Athens Panepistimioupoli, Ilisia 15701 HELLAS

ekarali@biosim.ntua.gr

Abstract: In this work we have assessed three subtraction techniques that use a different approach in order to calculate the scatter component and subtract it from the photopeak image: The Dual Energy Window Subtraction Technique (DEWST) the Convolution Subtraction Technique (CST) and a Deconvolution Technique (DT). All these techniques are compared to the standard method. The experimental results showed the superiority of DT, as a scatter correction technique.

Introduction

Small field of view detectors based on Position Sensitive Photomultiplier Tubes (PSPMTs) coupled to pixelized scintillators offer improved spatial resolution compared to the standard Anger camera and have been used in the last decade in dedicated small field of view systems for Single Photon Emission Computed Tomography (SPECT)[1][2]. Their main applications are planar and topographic imaging of small animals in laboratory environment and clinical scintimammography for the early detection of small breast tumors[3].

However SPECT images still suffer from low contrast as a result of photons scatter[4], mainly due to Compton effect, inside the patient or/and the detector. The application of an energy window around the central photopeak channel of each crystal cell is the standard method for excluding scatter component in pixelized scintillators, but small angle scattered photons still appear in the photopeak window. A number of scatter correction techniques have been proposed[4], however they have not yet been applied in pixelized scintillators. Further more there is a limited number of evaluation studies of different scatter correction techniques [4].

In this work we have assessed three subtraction techniques that use a different approach in order to calculate the scatter component and subtract it from the photopeak image: The Dual Energy Window Subtraction Technique (DEWST), the Convolution Subtraction Technique (CST) and a Deconvolution Technique. All techniques are compared to the standard method.

Materials and Methods

Data Acquisition: The gamma camera that was used is based on a Hamamatsu R2486 PSPMT, a parallel hole collimator (27.5mm thickness, with hexagonal holes 1.1mm in diameter) and a pixelized CsI(Tl) scintillator, 4.6cm in diameter, 4mm thick, with cell size 1.13x1.13mm^2. CAMAC electronics and a Macintosh computer are used for data acquisition and signal processing. PC controlled step-motor is used for object rotation in order to acquire tomographic data (Fig.1). The spatial resolution of the system has been measured and found <2mm in planar imaging [3]

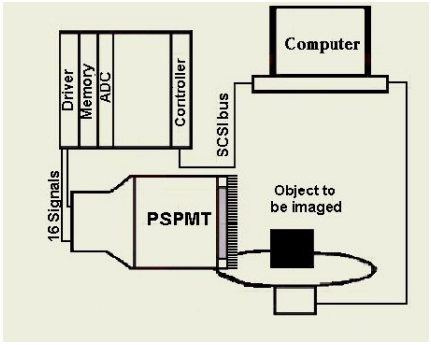

Figure 1: The acquisition system

A hot, a cold and a breast phantom have been used for the assessment of the three scatter methods. The hot phantom consisted of three capillaries 7cm long, with 1.5mm inner diameter and 1.6mm outer diameter, placed at 5mm and 7mm distances from each other and filled with a ^{99m}Tc solution, 8mCi/ml. The phantom was placed at a 10cm distance from the collimator inside a pot filled with 300ml of water. The phantom was imaged for 150secs and 301kcounts were acquired.

The cold phantom was a metallic cylinder with 1.5cm outer diameter, 0.8cm inner diameter and 0.7cm height, placed at the bottom of a thin plastic pot, 6cm in diameter and 8cm high. The pot was filled with 30ml of a ^{99m}Tc solution, 0.14mCi/ml, placed at a 10cm distance from the detector. The cold circular phantom was imaged for 3 minutes and 600kcounts were acquired.

The breast phantom consisted of two hot quantities of a ^{99m}Tc solution, both 0.5ml in volume, placed inside a pot, 10cm in diameter, containing a 300ml ^{99m}Tc solution, 2mCi/ml. The activity ratios of the hot spots to the background were 2:1 (S1) and 3:2 (S2) respectively.

ISSN: 1727-1983

The detector was placed at a 10cm distance from the bottom of the pot. The breast phantom was imaged for 16min and 790kcounts were collected.

Scatter correction methods: The Dual Energy Window Subtraction Technique (DEWST) proposed by Jaszczak et al. [5] involves data collection in a lower energy window, which provides a reasonable approximation for the scatter component in the photopeak window. Two images are used for scatter compensation; the photopeak image $P(\boldsymbol{u})$ and the lower energy window image L($\mathbf{u}$). If $C(\boldsymbol{u})$ is the corrected image then:

$$C(\boldsymbol{u}) = P(\boldsymbol{u}) - kL(\boldsymbol{u}) \qquad (1)$$

where $\boldsymbol{u}$ is the vector of image pixels coordinates and k is the weighting factor. The average optimal value for k was found to be equal to 0.5[5].

The Convolution Subtraction Technique (CST) proposed by Axelsson et al. [6] assumes that the scatter component in the photopeak window can be estimated as the convolution of the measured photopeak data $P(\boldsymbol{u})$ with a characteristic function $f(x)$ that can be modeled as an exponential function, which is derived from the system's Line Spread Function (LSF) in a scattering medium. In order to determine $f(x)$ a capillary 1.1mm inner diameter filled with a ^{99m}Tc solution was placed in the centre of a water filled cylindrical pot, 15cm in height and 10cm in diameter. Data were collected and line profile of the capillary activity was drawn. This line profile stands for the system's LSF. Using a least squares method, the one dimensional exponential function that best fitted the theoretically linear part of log(LSF) was:

$$f(x) = 0.0247e^{-0.07|x|} \qquad (2)$$

where x denotes distance in pixels from the centre of the camera's field of view (FOV).

Deconvolution techniques (DT) [7] assume that the measured data $P(\boldsymbol{u})$ derive from the convolution of the true data $C(\boldsymbol{u})$ and a characteristic two-dimensional function $h(\boldsymbol{u})$ that can be modelled as an exponential function. The latter is derived from the system's Point Spread Function (PSF) in a scattering medium:

$$P(\boldsymbol{u}) = C(\boldsymbol{u}) * h(\boldsymbol{u}) \qquad (3)$$

Various methods have been applied to solve (deconvolve) equation 3. We have used the blind deconvolution technique that is based on the Expectation Maximization (EM) Algorithm [8], which assumes that the true data $C_{k+1}(\boldsymbol{u})$, in a specific time $k+1$ is expressed as:

$$C_{k+1}(\boldsymbol{u}) = C_k(\boldsymbol{u})\{w(-\boldsymbol{u}) * \frac{P(\boldsymbol{u})}{w(\boldsymbol{u}) * C_k(\boldsymbol{u})}\} \qquad (4)$$

$$\text{with } w(\boldsymbol{u}) = FFT^{-1}\{\frac{FFT(h(\boldsymbol{u}))^*}{|FFT(h(\boldsymbol{u}))^2| + \gamma}\} \qquad (5)$$

where FFT denotes the Fast Fourier Transform and γ is the squared noise-to-signal ratio (NSR).

In our implementation of DT $h(\boldsymbol{u})$ was defined as:

$$h(\boldsymbol{u}) = 0.0247e^{-0.07|\boldsymbol{u}|} \qquad (6)$$

and the value of the parameter γ was experimentally determined as $\gamma = 0.0002$ for all cases.

Results

The results from the application of the three methods (one-photopeak, DEWST, CST and DT) are presented in Fig.1 and Tables 1-3. As it can be seen from the images and the corresponding line profiles, CST and DT offer significantly improved results when compared with the one- photopeak method. In particular the low-count regions and structures are better recovered after scatter compensation. CST and DT operate directly on projection data. Both assume a detector with as uniform response as possible. DEWST subtracts data corresponding to non photopeak photons and thus causes the highest reduction to the SNR.

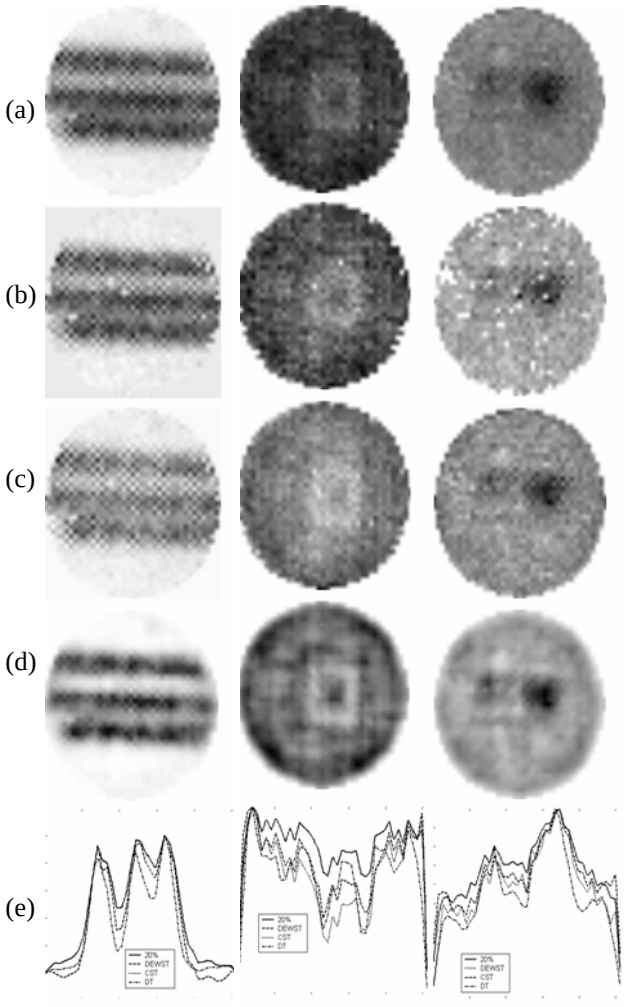

Figure 2: Hot (left column), cold (middle column) and breast phantom (left column) imaging. (a) The image in the 20% photopeak window. (b) The corrected image using DEWST. (c) The corrected image using CST. (d) The corrected image using DT. (e) Normalized line profiles.

ISSN: 1727-1983

Table 1: Image contrast using three different ratios for ROIs in the cold (C) and background (B) region for the standard 20% photopeak window technique, DEWST, CST and DT.

Method	C/B	(B-C)/B	(B-C)/(B+C)
	0.7498	0.2502	0.1430
DEWST	0.6466	0.3534	0.2146
CST	0.5399	0.4601	0.2988
DT	0.5547	0.4423	0.2839

Table 2: Image contrast using three different ratios for ROIs in the spot with ratio to background 2:1 (S1) and the background (B) region for the standard 20% photopeak window technique, DEWST, CST and DT.

Method	S1/B	(B-S1)/B	(B-S1)/(B+S1)
20%	1.3881	0.3881	0.1625
DEWST	1.6191	0.6191	0.2364
CST	1.5113	0.5113	0.2036
DT	1.8191	0.8191	0.2906

Table 3: Image contrast using three different ratios for ROIs in the spot with ratio to background 3:2 (S2) and the background (B) region for the standard 20% photopeak window technique, the DEWST, CST and DT.

Method	S2/B	(B-S2)/B	(B-S2)/(B+S2)
20%	1.1326	0.1326	0.0622
DEWST	1.2319	0.2319	0.1039
CST	1.1758	0.1758	0.0808
DT	1.3898	0.3898	0.1631

Discussion

The necessity for pixelized scintillators in dedicated SPECT systems that are based on PSPMTs is uncontested since the thickness of the PSPMT glass window together with a large intrinsic spread of charge distribution hamper the use of planar scintillation crystals [2]. In addition the use of a thick crystal with good detection efficiency involves a large spread of light distribution with respect to the size of the PSPMT that decreases spatial resolution [9]. Scatter correction has not been extensively investigated and the use of an energy window around the photopeak channel of each crystal cell is a simple technique, which does not reject the scatter component that is included in the photopeak.

The DEWST uses the energy of each detected photon in order to determine weather it is located in the selected lower energy window or not. The assumption that this window can be used in order to provide an estimate for the scattered photons in the primary photopeak window is independent from the acquisition mode (planar or topographic). The DEWST, as it has been modified, is related to the pixelized scintillators physics since it uses the energy spectrum of each crystal cell. All system's non-uniformities do not affect the method since calibration is performed in pixel level and the method is applied in pixel level as well. Each crystal cell is treated as an independent detector with uniform response and in the case of the used crystal, the response of the system is considered to be uniform only within each pixel, which has an area of 1.13x1.13mm^2. However this method subtracts non-photopeak data from photopeak data thus reducing image quality, as it can been seen in Fig. 1(b).

The CST uses a function $f(x)$ that depends on the properties of the detection system to be used. Since this function is desirable to be independent of the position of the source within the investigated object, the line source was placed at 10 different distances from the detector. The used parameters of the function $f(x)$ where the mean values of the 10 different parameters estimated for each corresponding distance. The obtained results were superior, when compared with the standard one-photopeak window method, as it is shown in tables I-III. However a unique function $f(x)$ that could produce optimum results for different imaging systems could not be determined.

DT seems to drastically reduce scatter component and increase image contrast. Moreover DT compensates for any factor that decreases image contrast and resolution, like the collimator sensitivity. In Fig.2 we have applied DT in homographic images of a small animal (small mouse) head. As it can be seen from Fig.2b DT causes a significant scatter reduction and improves image contrast. On the other hand DT like CST depends on the used energy window and system's energy resolution. The major drawback of DT is that the used algorithm is sensitive to the initial image estimate and can exhibit instability

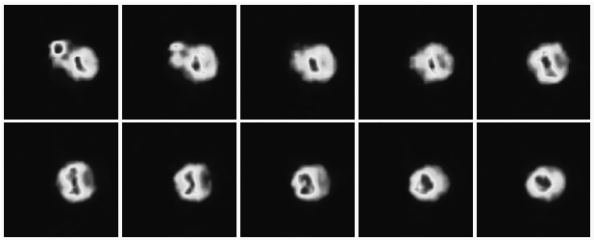

(a)

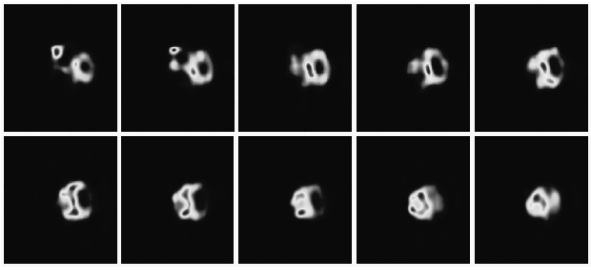

(b)

Figure 3. Tomographic images of a small animal head. a)The images in the 20% photopeak window, b) the corrected images using DT.

ISSN: 1727-1983

Conclusion

The presented results indicate that the three used techniques (DEWST, CST and DT) can play a very important role in scatter rejection in scintillator array detectors. Scintimmamography is a research area where these methods would improve image contrast and allow the early detection of small tumors.

Acknowledgments

The authors would like to thank S. Majewski and D. Weisenberger from "Jefferson Lab" and R. Pani from Univeristy of Rome "La Sapienza" for offering part of the used equipment and their experience.

References

[1] WEISENBERGER A.G. [et. al]. , (1998): 'Design features and performance of a CsI(Na) array based gamma camera for small animal gene research', IEEE Trans Nucl Sci. Vol. 45, 1998, pp 3053-3058

[2] PANIM R. [et. al], (2002): 'Scintillation arrays characterization for photon emission imaging, Nuclear Instruments and Methods in Physics Research Section A: Accelerators, Spectrometers, Detectors and Associated Equipment', Vol. 477, Issues 1-3, 21, 2002, pp 72-76

[3] LOUDOS, G. K.; NIKITA, K.S. ; GIOKARIS, N.D. [et. al] , (2003): 'A 3D High Resolution gamma-camera for Radiopharmaceutical Studies with Small Animals', Applied Radiation and Isotopes, Volume 58, Issue 4, 2003, pp 501-508

[4] ZAIDI, H.; KORAL, K.F. , (2004): 'Scatter modeling and compensation in emission tomography', Eur J Nucl Med Mol Imaging(31), Springer-Verlag, 2004, pp 761-782

[5] JASZCZAK, R.J. [et. al] , (1984): 'Improved SPECT Quantification Using Compensation for Scattered Photons', J. Nuc. Med., Vol. 29, 1984, pp.893-900

[6] AXELSSON, B.; MSAKI, P. ; ISRAELSSON, A. , (1984): 'Subtraction of Compton-Scattered Photons in Single-Photon Emission Computed Tomography', *J. Nuc. Med.*, Vol. 25, 1984, pp.490-494

[7] MIGNOTTE, M. ; MEUNIER, J. ; SOUSY, J. ; JANICKI, C. , (2002): 'Comparison of deconvolution techniques using a distribution mixure parameter estimation: Application in single photon emission computed tomography imagery', Journal of Electronic Imaging, SPIE, Vol. 11, No. 1,2002

[8] SHEPP L.A AND VARDI Y, (1982): 'Maximum likelihood reconstruction for emission tomography', IEEE Trans. Med. Imaging Vol. MI-2, 1982, pp.113-122

[9] KIM, J.H. [et. al] , (2000): 'Development of a Miniature Scintillation Camera Using an NaI(Tl) Scintillator and PSPMT for Scintimammography', Physics in Medicine and Biology, Vol. 45, Issue 11, 2000, pp.3481-3488

ISSN: 1727-1983